Chapter 11
Fire Spread

Abstract Fire spread is a very important issue during fires in tunnels. The elongated geometry of a tunnel with a relatively low ceiling height makes the flames and hot gases follow the ceiling over long distances, increasing the risk for fire spread. The use of ventilation in the tunnel as well as different types of vehicles, commodities, and materials influences the fire spread. This chapter contains both a summary of traditional ignition and fire spread theory and experiences especially related to situations in tunnels with risk for fire spread. Different aspects of spread and burning of liquids are presented and discussed.

Keywords Fire spread · Ignition · Radiation · Ignition temperature · Spill fire

11.1 Introduction

Fire spread is one of the most important processes during fires in tunnels. In many cases it determines the duration of a fire, the hazards for the evacuees and the possibilities for the fire and rescue services to fight the fire. As soon as the fire has spread to more than one vehicle, the situation becomes more severe. This is especially true when heavy goods vehicles (HGVs) are involved.

Rew and Deaves identified five different types of mechanisms for fire spread between wagons in a rail tunnel [1]:

1. Flame impingement
2. Flame spread (that is, flame spread across a surface)
3. Remote ignition/"flashover." Here they discussed spread from one wagon to another due to flashover. In many cases this means ignition by radiation. It also includes convective heating leading to auto ignition despite the fact that this may be combined with heating by radiation from flames, hot gases, or hot surfaces.
4. Fuel transfer. This includes both spread by burning liquid and by burning debris ("fire brands") transported downstream of the fire.
5. Explosion, which can spread fuel and fire.

Flame impingement relates to what is termed piloted ignition. There are two types of piloted ignition: (1) a pilot flame impinging directly on the surface, which is

H. Ingason et al., *Tunnel Fire Dynamics,* DOI 10.1007/978-1-4939-2199-7_11

heated by convection and/or radiation and (2) a pilot flame (or spark) in the gases near the surface, but without heating the object. For fire spread between vehicles in a tunnel, the first type of piloted ignition is the dominating process, while the second type can be involved in the first ignition process.

An extended flame along the ceiling in a tunnel is an important factor to consider when studying fire spread in a tunnel. It will influence both mechanisms 1 and 3. It can also increase the flame spread along a surface (mechanism 2). Therefore, it is important to be able to estimate the flame length in different fire situations in tunnels. This subject is extensively discussed in Chap. 9.

11.2 Introduction to the Theory of Ignition

11.2.1 Solids

Fire spread can be seen as a sequence of ignition processes and, therefore, an introduction to the theory of ignition is given here. For solids there are a number of different types of ignition [2]:

1. Ignition of fuel vapors from the material.
2. Smoldering ignition. An example of this is self heating of a porous material.
3. Direct ignition of the surface of a solid material. An example of this is ignition of some metals.
4. Ignition by a chemical reaction taking place directly in the solid phase. An example of this is explosives and pyrotechnics

Ignition type 1 is the most common type for solids and for fire spread in tunnels. The process of producing fuel vapors is often called pyrolysis, that is, the breakage of large molecules to smaller molecule fragments that can be released as gases. Some materials vaporize without pyrolizing. For ignition to take place, the material needs to be heated enough to produce gases in concentrations suitable for ignition. The fuel vapors then need to mix with air (or other oxidizer) to form a flammable mixture. This means that ignition can take place first after the production of fuel vapors is such that the concentration of the mixture reaches above the lower flammability limit (LFL). A schematic drawing of heat and mass transfer in solid materials is presented in Fig. 11.1.

For ignition to occur, the temperature of the fuel/air mixture needs to be increased to obtain an auto-ignition. Alternatively, an external heat/energy source can be applied to the mixture, for example, a spark or a flame. This is called piloted or forced ignition. If a material is affected by external heating, the ignition in most cases (for most solids) takes place in the gas phase. The heat drives off volatiles, which then burns outside the material.

One parameter often used to define or characterize the ignition properties of a material is the ignition temperature. The ignition temperature is, however, defined

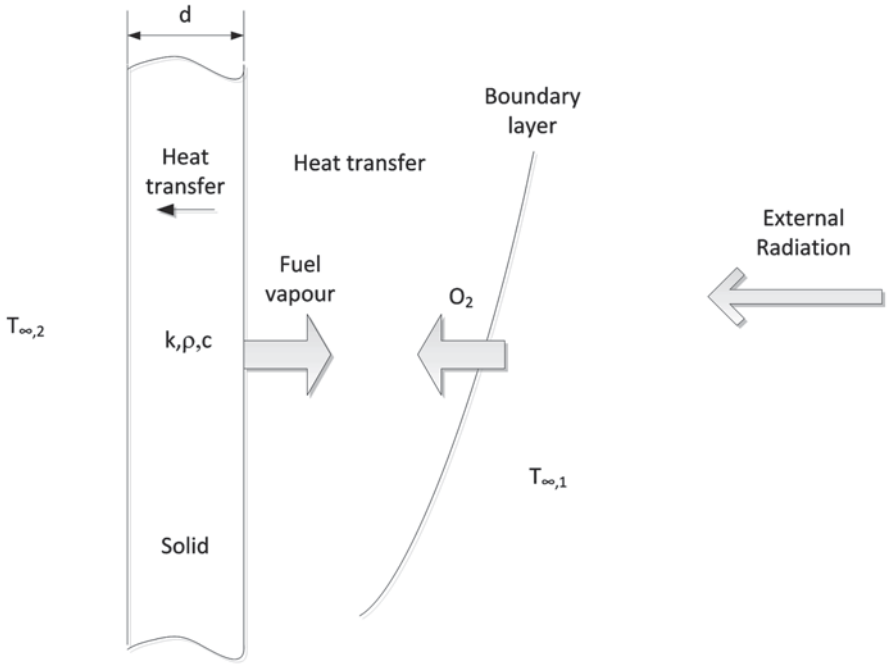

Fig. 11.1 Simplified schematics of the processes involved in ignition of a solid

mainly in two different ways depending on the situation. First, in fire testing situations the furnace temperature is often used, for example, the gas temperature near the object needed for the specimen to ignite. Second, in many studies the surface temperature of the specimen at the time for ignition is used. The problem with the latter definition is that the surface temperature is often very difficult to measure.

The first definition is convenient to use for studies of the ignition temperature using furnaces with homogenous gas temperature. It is, however, important to note that when tested in a furnace, the surface temperatures of the object and the gas temperature in the furnace are not necessarily the same. There are, however, measurements of the temperatures at the surface and in the gas phase right before ignition and in these cases these temperature were essentially the same [2]. Another important issue is that in a real case the conditions may be such that the fuel is heated by radiation but cooled by convection, that is, there is no homogenous high-temperature media surrounding the fuel. Irrespective of whether small thermocouples or optical methods are used to measure the surface temperature there are risks for significant errors, for example, that the thermocouple is not measuring exactly at the surface and the surface temperature of the material or that the optical properties (emissivity) of the material are not known all through the process of heating the surface. The surface temperature at ignition also depends on whether the material is thermally thin or thick.

Thermally thin means that the material is physically thin or has high thermal conductivity (k) so that it can be assumed that the temperature is the same throughout the material. The basic theory can be found in Chap. 10 on heat fluxes and thermal resistance. To distinguish the thermally thin materials from thermally thick materials, one can introduce the Biot number, which is defined as:

$$Bi = \frac{hd}{k} \tag{11.1}$$

where h is the heat transfer coefficient (kW/(m^2 K)), d is the thickness (m) of the material (see Fig. 11.1) and k is the thermal conductivity (kW/(m K)). For Bi smaller than 0.1, the material is considered thermally thin. This means that the conduction of heat inside the object is much faster than the convective heat transfer at its surface. This means that a uniform body temperature can be assumed and this is often referred to as the *lumped heat capacity* model.

Fire scenarios, for example, with significant radiation and high levels of irradiance, often involve only short time scales of the heat transfer mechanisms which are relevant for the important processes. This means that only the surface can be assumed to be important for the ignition process. In these situations the materials are said to be thermally thick and can approximately be treated as a semi-infinite plate. This means that when the front side of a material is heated, for the time of consideration a significant temperature rise has not occurred at the back side. The parameters important for determining whether a material is to be considered thermally thick are the thermal properties of the material (k, ρ, c), the thickness of the material and the time of interest, where ρ is the density (kg/m^3) and c is the heat capacity (kJ/(kg K)). One way of expressing this is by calculating the thermal penetration depth, δ_p (m). This is used to calculate how far the heat wave has reached into the material and is expressed as distance reached where a certain fraction of the temperature rise is reached in relation to the surface temperature rise. Wickström [3] gave two such penetration depths relating to a relative temperature rise of 5 and 1 %, respectively:

$$\delta_{p,0.05} = 2.8\sqrt{\alpha t} \tag{11.2}$$

and

$$\delta_{p,0.01} = 3.6\sqrt{\alpha t} \tag{11.3}$$

where α is the thermal diffusivity ($\alpha = k/(\rho c)$; m^2/s) and t is the time (s).

This means, of course, that the penetration depth depends on how it is defined and what relative temperature rise is used.

Irrespective of which one is selected, one should remember that they are developed for a situation with single-sided heating and that the penetration depth for a case with heating from both sides needs to be less than half of the corresponding value calculated from the single-side equation.

Whether a composite material with a thin outer layer should be considered thermally thin or thick depends on the density of the substrate or material behind the

outer layer. With a much lower density of the material behind, the ignition behavior is determined by the outer layer alone, while a substrate with high density can make the composite thermally thick even if the substrate is incombustible.

Note that most fuels present in vehicles are thermally thin. Babrauskas [2] gives a rule of thumb that products with thickness ≤ 1 mm will be thermally thin while products with a thickness ≥ 20 mm will be thermally thick (foam materials are excluded from this generalization).

The behavior of a material also depends on the heat flux. For a very high irradiance it can behave thermally thick, while for low irradiance it can behave thermally thin.

To complicate things, the ignition is not only controlled by the surrounding temperature and the ignition temperature but also the geometry and thermal inertia of the fuel, that is , how the heat is transferred into the object. This also depends on the properties of the heating source, for example, the level of radiation. It is important to note that in many cases the time to ignition is what is of specific interest. In these cases, the thermal inertia may play a more significant role than the ignition temperature. The time to ignition for thick homogenous objects is proportional to the thermal inertia. The thermal inertia is dependent on the heat conductivity (k), density (ρ), and specific heat capacity (c). In the literature, one can find two different definitions:

$$I_1 = k\rho c \tag{11.4}$$

$$I_2 = \sqrt{k\rho c} \tag{11.5}$$

In this chapter the first definition ($kJ^2/(s\ m^4\ K^2)$) has been used when presenting data in different tables. Values of heat conductivity, density, specific heat capacity, and thermal inertia for some selected materials are presented in Table 11.1.

The exact ignition temperature varies depending on apparatus used for the measurement. However, the temperature for piloted ignition is lower than the corresponding auto-ignition temperature. Examples for this are presented by Babrauskas for thermoplastics with ignition temperature of 369 °C (+/− 73 °C) for piloted ignition and 457 °C (+/− 63 °C) for auto-ignition. The corresponding average ignition temperatures for thermosetting plastics are given as 441 °C (+/− 100 °C) and 514 °C (+/− 92 °C) [2]. There are also examples where the measured ignition temperature (for wood) was higher than the measured furnace temperature which means that self heating occurred.

It has been observed that the surface temperature for wood at ignition depends on the situation [5, 6]. This is summarized in Table 11.2.

To exemplify the influence of the thermal inertia on the ignition of a solid, some material and ignition properties of expanded polystyrene (EPS) will be discussed. In Table 11.3 results from cone calorimetry tests with different types of EPS are presented [2, 7, 8] and are also compared with some other selected materials.

Table 11.1 Material properties of some selected solid materials [3, 4]

Material	Heat conductivity, k (kW/(m K))	Density, ρ (kg/m^3)	Specific heat capacity, c (kJ/(kg K))	Thermal inertia, $k\rho c$ (kJ^{2}m^{-4}s^{-1}K^{-2})
Polyurethane foam	0.0003	20	1.400	0.000840
Fiber insulating board	0.00004	100	2.000	0.007920
Wood, pine	0.00014	500	2.800	0.196000
Wood, oak	0.00017	700	2.800	0.333000
Gypsum plaster	0.0005	1400	0.840	0.588000
Concrete	0.0017	2300	0.900	3.53
Steel (mild)	0.046	7850	0.460	166
Aluminum	0.20	2700	0.900	486
Copper	0.39	8930	0.390	1360

Table 11.2 Surface temperature for wood at ignition [5, 6]

Mode of heat transfer	T_s, spontaneous ignition (°C)	T_s, pilot ignition (°C)
Radiation	600	300–410
Convection	490	450

The time to ignition for a material exposed to radiation depends on the level of radiation, that is, with increasing radiation the ignition time decreases. At the other end of the scale, the ignition time increases so that below a certain radiation level ignition does not occur, at least not within a specific and long time period of exposure. This minimum heat flux, $\dot{q}''_{\min}$ (kW/m^2), is defined as the minimum heat flux needed for the surface temperature to reach the ignition temperature, T_{ig} [2], which can be determined experimentally for different materials. Cleary and Quintiere [8] performed tests in a cone calorimeter and found that $\dot{q}''_{\min}$ was 15 kW/m^2, for polystyrene foam, both expanded and extruded, fire retarded and nonfire retarded. In another study, also with the cone calorimeter, Dillon [7] analyzed two different fire retarded polystyrene foams, for example, EPS and reached $\dot{q}''_{\min}$ of 8 and 23 kW/m^2, respectively. At a first glance at the values in Table 11.3 it appears to be that 15 kW/m^2 could be used as a representative value of $\dot{q}''_{\min}$ irrespective of type of EPS. However, in the two test series the thermal properties of the materials differed, that is, the thermal inertia ($k\rho c$) was different. This could explain why the fire-retarded and the nonfire retarded materials showed the same $\dot{q}''_{\min}$ in the work by Cleary and Quintiere. As can be seen in Fig. 11.2, there is a large difference in the correlation whether the nonfire retarded value is included or not. If the nonfire retarded value is left out, the following expression can be used:

$$\dot{q}''_{\min} = 27.2 \cdot \left(k\rho c\right)^{-0.5} - 13.4 \tag{11.6}$$

Table 11.3 Results for cone calorimetry tests with expanded polystyrene (EPS). Some other materials are included for comparison [2, 7, 8]

Material	Thickness, mm	ρ, kg/m^3	$k\rho c$, kJ^{2}m^{-4}s^{-1}K^{-2}	T_{ig}, meas, °C	T_{ig}, comp[a], °C	$\dot{q}''_{min}$, kW/m^2	References
Polystyrene foam, EPS	50	32	0.58		376	15	[8]
Polystyrene foam, FR EPS	50	16	0.96		376	15	[8]
Polystyrene foam, FR EPS	50	32	0.91		376	15	[8]
Polystyrene foam, FR EPS	40	30	1.594		295	8	[7]
Polystyrene foam, FR EPS	80	30	0.557		490	23	[7]
Polystyrene foam, FR XPS	50	32	0.91		376	15	[8]
Polyethene			1.834	315–330	300		[9]
PVC, FR	3	1505	1.306		415	16	[7]
Wood, beech	15	749	0.504		358		[10]
Wood, beech 9% MC			0.463	380			[11]
Wood, Douglas fir 0% MC	16.8	465	0.159	350			[12]
Wood, mahogany			0.512		407	18	[2, 13]
Wood, Monterey pine 0% MC	17.5	460	0.156	349			[12]
Wood, Monterey pine 11% MC			0.593	340			[11]
Wood, oak			0.447		301		[2, 14]
Wood, spruce	15	468	0.208		375		[10]
Wood, spruce			0.214		358		[15]
Wood, spruce			0.181		352		[2, 14]

[a] Computed ignition temperature

Since the ignition temperature can be difficult both to define and measure, other means for comparing ignition conditions for different materials have been studied. One such parameter is the mass loss rate at ignition. However, it can also be difficult to measure this accurately at ignition and the values can be apparatus dependent

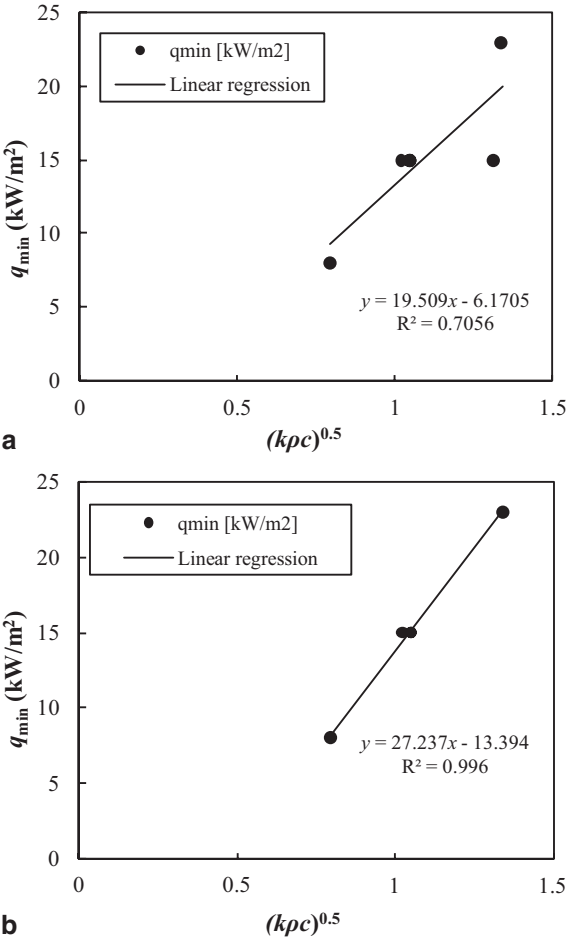

Fig. 11.2 Minimum heat flux for ignition of EPS as function of thermal inertia. In the *upper* Figure (**a**) there is an outlier corresponding to a non-fire retarded case. If this outlier is removed the correlation is much better as can be seen in the *lower* Figure (**b**)

[2]. Another parameter that could be useful is the heat release rate (HRR), where a span between 25 and 50 kW/m^2 are given for some common materials at piloted ignition [2].

The geometry of the object and the position of the heat source (flame) are important since it is easier to ignite a corner than an edge or a flat surface. The reason for this is that in the case with a corner the surface temperature is raised more quickly since the heat can flow into the body along three directions [2]. A vertical surface will in most cases ignite at the top. There are two reasons for that: First, a convective flow will be formed along the surface. At ambient temperature, this flow will cool the surface. The boundary layer will be thicker at the top, reducing the cooling. For fires in tunnels in most cases the heating will also come from the hot gases and flames along the ceiling, heating the surfaces from above. Second, for a very high radiation, the effect of convection on ignition will be negligible. If a large surface is exposed to radiation, the time to ignition will be shorter than the time to ignition for a small surface for a given irradiance.

Another phenomenon that can influence the ignition is charring. This process can both increase ignition time and increase the critical heat flux below which ignition will not take place.

A third mechanism for ignition, in addition to radiative and convective heating, is direct contact with a hot body. It has been shown, however, that this requires significantly higher ignition temperatures (around 600 °C for several materials) than both piloted and auto-ignition.

Effect of Velocity Air flow can affect ignition and fire spread in several different ways. If a material is heated by radiation, a flow of air at relatively low temperature cools the object and the gases near the material by convection. It also dilutes the fuel/air mixture. An air flow leads in these cases to a higher ignition temperature needed for ignition compared to a case with lower velocity or without forced airflow. This effect is highest at the lowest irradiances leading to ignition.

If the air flow has a temperature leading to convective heating, there is an optimum velocity leading to the shortest ignition time. For low velocities, an increased velocity leads to faster pyrolysis and better mixing and in turn faster ignition, while at higher velocities an increased velocity decreases the residence time and thereby the time for chemical reaction. As for cold flows, it also dilutes the fuel vapors. There is a limit for the velocity above which ignition will not occur. This limit depends on the temperature and oxygen concentration.

If the geometry is three dimensional and complex or if the material is ignited in the glowing mode, the addition of air via an increased air flow will affect the ignition, increase the reaction rate, and increase the rate of flame spread. The reason for this is that it can be difficult for the air (oxygen) to reach the pyrolysates and the combustion zone. This can be the case in a tunnel fire when an increased air flow can make it easier for the air to reach the combustion zone in for example an HGV cargo.

In a tunnel, an airflow can also tilt the flames in such a way that they are either closer to a combustible surface or forced into a three-dimensional fuel. In both these cases it will increase the flame and fire spread. There are also other situations where an increased velocity will decrease the size of a fire. The effect of the ventilation on the fire size is discussed in more detail in Chap. 4.

11.2.2 Liquids

Combustible liquids are in tunnels available in different form, both as fuels for the individual vehicles and as goods transported in large bulk volumes. Therefore, it is important to understand also the ignition of liquids. In most cases the materials do not ignite in the form of liquid, but instead in the form of vapors mixing with the air, forming a combustible mixture. Liquids are also classified according to their flash point, that is, the lowest temperature at which a liquid can produce enough vapors to form a flammable vapor/air mixture. It should be noted that there are different test methods for determining the flash point, for example, closed cup or open cup flash point, and that these do not give the same values. Flash points for some selected

Table 11.4 Flash point and fire point temperatures for liquid fuels [2, 5]

Material	Closed cup flash point (°C)	Open cup flash point (°C)	Fire point (°C)
Gasoline (100 Octane)	−38[a]		
n-Hexane	−22[a, b]	−26[b]	
Cyclohexane	−20[a]		
n-heptane	−4[b]	−1[b]	2[b]
n-octane	12[b], 13[a]		
Iso-octane	−12[a]		
n-nonane	31[b]	37[b]	42[b]
n-decane	46[a], 44[b]	52[a, b]	61.5[a, b], 66[b]
n-dodecane	74[a, b]		103[a, b]
m-xylene	25[b]		44[b]
o-xylene	32[b]	36[b]	42[b]
p-xylene	27[a], 25[b]	31[a, b]	44[a, b]
Methanol	11[a], 12[b]	1[a] (13.5)[a, c]	1[a] (13.5)[a, c]
Ethanol	13[a, b]	6[a], (18)[a, c], 22[b]	6[a] (18)[a, c], 22[b]
Propanol	26[a], 29	16.5[a] (26)[a, c]	16.5[a] (26)[a, c]
n-butanol	35[a]	36[a, b] (40)[a, c]	36[a] (40)[a, c], 36–50[b]
Sec-butanol	24[b]		29[b]
i-pentanol	41[a]		57[a]
Glycerol	160[b]		207[b]
JP6		38[b]	43[b]
Fuel oil, No. 2	124[b]		129[b]
Fuel oil, No. 6	146[b]		177[b]
Motor oil	216[b]		224[b]

[a] Drysdale [5]. Closed-cup flash points comes from work by NFPA [16], while the open-cup flash point and fire points come from work by Glassman and Dryer [17]
[b] Babrauskas [2]
[c] Values in parentheses refer to ignition by a spark and not pilot flame

liquid fuels are presented in Table 11.4. Since the processes are different, there is no relation between the flash point and the auto ignition temperature. The fire point, which is also included in Table 11.4, is the lowest temperature for which ignition leads to sustained burning.

A burning liquid fuel can constitute a hazard in itself, but also be an important source for fire spread to other vehicles. An important parameter is also the thickness of the fuel; either it is burning on the road surface or in a bulk transport. The effects of the boundaries underneath the fuel bed are important but are seldom considered as a parameter that can influence the burning conditions.

11.2.2.1 Release of Liquids

Liquid fuels can be released in tunnels in different ways: small leakages from fuel tanks or fuel hoses, ruptured tanks, leakage from a tanker carrying a flammable liquid, etc.

To estimate the extent of an unconfined spread of a liquid fuel, one needs to know the resulting thickness of the spill. Gottuk and White [18] summarize the results from several tests in the following relationships:

$$\begin{cases} A/V_s = 1.4 \text{ m}^2/\text{L Spill} < 95 \text{ L} \\ A/V_s = 0.36 \text{ m}^2/\text{L Spill} \geq 95 \text{ L} \end{cases} \tag{11.7}$$

where A is the area (m^2) and V_s is the volume in liters (L) of the spill

As conservative minimum depths δ (mm), the following values were given:

$$\begin{cases} \delta = 0.7 \text{ mm} \quad \text{Spill} < 95 \text{ L} \\ \delta = 2.8 \text{ mm} \quad \text{Spill} \geq 95 \text{ L} \end{cases} \tag{11.8}$$

When the area of unconfined spill is calculated it is important to note that the area increases after being ignited. That means if cold spill area is denoted A_s, the fire area, A_f, can be calculated as [18]:

$$A_f = 1.55 A_s \tag{11.9}$$

The discussion above, regards a momentary release of a certain volume of fuel. If there is continuously flowing spill, the situation will be different. After ignition a balance will be reached between the volumetric burning and flow rates of the liquid release, $\dot{V}_L$ (m^3/s). From this balance a steady state diameter, D_{ss} (m) can be derived [18]:

$$D_{ss} = \left(\frac{4\dot{V}_L \rho}{\pi \dot{m}''} \right)^{1/2} \tag{11.10}$$

Based on empirical data, Gottuk and White recommend that for high fuel release rates (>10 L/min), confined pool burning rates are used, while for lower rates spill burning rates are used, that is, one fifth of the pool burning rates. Burning rates in kg/(m^2 s) for pool fires are discussed in more details in Chaps. 3 and 4.

Ingason [19] performed spillage tests on roadway asphalt and painted particle board with different slopes, leakage hole diameter, and volume flow rates.

The volume flow rate, $\dot{V}$ (m^3/s), of a leakage from a circular hole in a vehicle trailer tank can be calculated from:

$$\dot{V} = 2A_T K(\sqrt{h_1} - Kt) \tag{11.11}$$

where

$$K = \frac{C_v \pi D^2 \sqrt{2g}}{8A_T} \tag{11.12}$$

and A_T is the horizontal surface area of the leaking compartment (m^2), D is the hole diameter of the leakage (m), h_1 is the initial height (m) of the fuel (gasoline) at $t=0$ s, C_v is the flow contraction coefficient (=0.7), g is gravitational acceleration (m/s^2) and t is the time (s).

Ingason found that the area of the spill can be estimated by

$$A = BL \tag{11.13}$$

where B (m) is an average width between the impingement point of the leakage and the side where the drainage system is and L is the center line distance from the impingement point to the drainage system (m). The test results showed that for a spill onto asphalt B can be estimated by the following empirical correlation:

$$B = 48\dot{V}^{0.46} \tag{11.14}$$

The length L depends on the slope but Ingason gave an expression for the maximum spillage area [19]:

$$A_{\max} = \frac{\dot{V}\rho_f}{\dot{m}''} \tag{11.15}$$

where ρ_f is the density of the fuel (kg/m^3) and $\dot{m}''$ the burning rate of the spillage ($kg/s/m^2$). For a circular pool spillage with a diameter D_{ss}, Eq. (11.15) gives the same results as Eq. (11.10). The actual spillage area depends on the design of and distance to the drainage system.

Example 11.1 A tanker carrying 20,000 m^3 of gasoline starts to leak through a pipe connected to one of the five tanker compartments. The surface area A_T of each compartment is 3 m^2. The diameter of the leaking opening is 0.05 m and the distance to the drainage system is 6 m. What is the potential fire size, or HRR (in MW) on the road surface if the fire starts after 30 s?

Solution: As there are five compartments, each carries 4 m^3 of gasoline. The initial height h_1 is therefore $4m^3/3m^2 = 1.33$ m. Using Eq. (11.12) *and $C_v = 0.7$ we obtain $K = 0.001$ and with aid of* Eq. (11.11)*, we obtain the volume flow after 30 s, $\dot{V} = 0.0067$ m^3/s (6.7 l/s or 405 l/min). The width B of the spillage at this time is obtained by using* Eq. (11.14)*, or 4.8 m. The total area A is obtained by* Eq. (11.13)*, or 28.8 m^2. The maximum spillage area A_{max} that can exist is obtained with* Eq. (11.15)*. From* Table 11.4 *we obtain for gasoline $\rho_f = 740$ kg/m^3, $\dot{m}'' = 0.055$ $kg/(m^2\,s)$ and $\Delta H_{c,eff} = 43.7$ MJ/kg (assuming $\chi = 1$). The maximum area that can burn is $0.0067 \times 740/0.055 = 90$ m^2 which is larger than 28.8 m^2. Thus, the HRR will be $28.8 \times 0.055 \times 43.7 = 69$ MW. Here we have not considered the effects of pan size or the depth of the fuel.*

11.2.2.2 Flame Spread over a Liquid Surface

It has been shown that both the flame spread rate and the fire intensity decreases significantly when the fuel depth decreases below a couple of centimeters [18, 20].

In tests on JP-5 fuel, the HRR for a thin fuel layer was 20–25 % of the HRR for the thick-layer case [20]. There are also studies indicating that the flames do not spread from the source of ignition when the fuel layer thickness is below 1.5 mm [20].

The spreading rate of a fire over a liquid fuel surface depends on the temperature of the fuel. Above a certain initial surface temperature the flame spread is controlled by the gas phase and flame propagation velocities in the order of 1 m/s can be observed [18]. Below that temperature, different regions were observed. The different temperature intervals and the observed velocities might vary between fuels and setup, but the effect of the fuel temperature is clear from the reported experiment. It is also important to remember that the flame spread rate decreases with the pan width [20].

White et al. [20] studied the effect of the temperature on the flame spread rate, but for isopentanol. They also observed a significant increase in the flame spread when the liquid temperature increases. As the temperature increased, three different regions were identified: the liquid-controlled, the gas phase-controlled, and the asymptotic gas phase-controlled regions. In the first region (I), where the flame is spread with surface tension-induced flow, there is a slow increase in flame spread rate with temperature. In the second region (II) there is a steep increase in flame spread rate with temperature while in the third region (III) the flame spread rate is approximately constant with increased temperature (see Fig. 11.3). The transitions between the different regions occur at the temperatures T_{go} and T_{gm}, respectively. The regions are defined in Fig. 11.3.

The experimental results indicate that the parameters most important for the flame spread are the initial fuel temperature (before ignition), T_l, the flash point of the fuel, T_{fl}. and the difference between them. For JP-8, for example, the transition between region I and region II occurred when $T_l - T_{fl} = T_{go} - T_{fl} \approx 18\,°C$. The results for different fuels are summarized in Table 11.5. Flash points for other fuels are given in Table 11.4.

For hydrocarbons tested, the maximum flame-spread rate in region I was 0.1 m/s and in region III between 1.20 and 2 m/s. This was the case also for alcohols, but there the span limits in region III were 1.5 and 2 m/s. When the flame spread rate is known, the fire area can be described:

$$\begin{cases} A_f = \pi v^2 t^2 \text{ (circular flame spread)} \\ A_f = wvt \text{ (rectangular flame spread)} \end{cases} \tag{11.16}$$

where v is the flame spread velocity (m/s) and w is the width (m) of the confinement of the fuel, for example, walls.

The burning rate of a spill fire is lower than the corresponding confined pool fire with a significantly larger fuel depth (centimeters rather than millimeters). For diameters larger than 1 m, the burning rate of a spill fire is approximately one fifth of the burning rate of the corresponding confined pool fire [18].

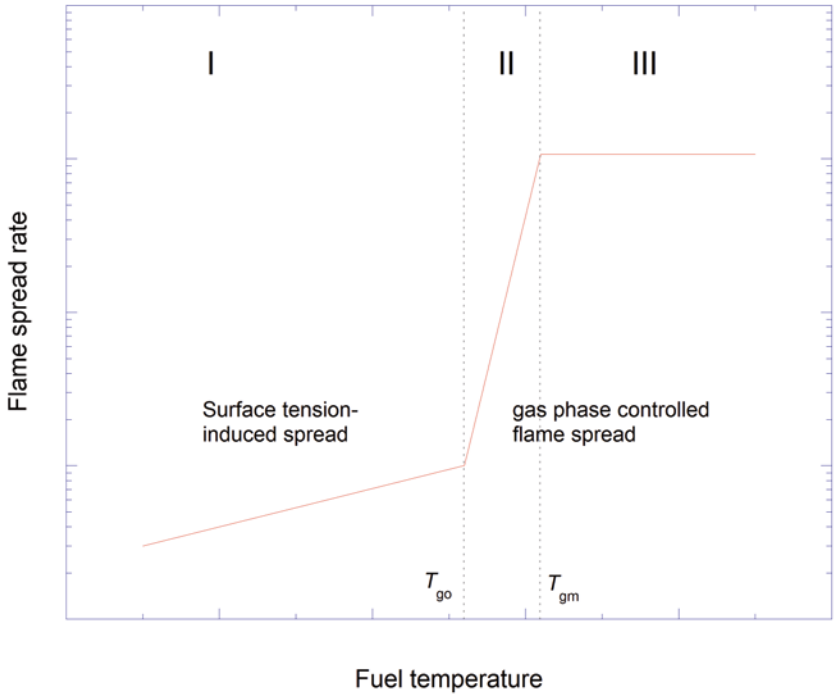

Fig. 11.3 Presentation of the regions of flame spread as function of fuel temperature and definition of T_{go} and T_{gm}. (After Gottuk and White [18])

Table 11.5 Summary of transition temperature between different regions for some selected fuels [18]

Fuel	T_{fl} (°C)	T_{go} (°C)	$(T_{go}-T_{fl})$	T_{gm} (°C)	$(T_{gm}-T_{go})$	$(T_{gm}-T_{fl})$
JP-8	39	57	18	62	5	23
25/75 JP-8/5	42	60	18	66	6	24
50/50 JP-8/5	48	65	17	72	7	24
75/25 JP-8/5	54	68	14	74	6	20
JP-5	63	76	13	79	3	16
Decane	44	56	12	62	6	18
Average of 1–6 above			15		6	21
1-Pentanol	48	52	4	62	10	14

11.2.2.3 The Effect of Macadam

The burning rate of a liquid fire depends on the depth of the fuel layer. The effects of different thicknesses on the HRR have been discussed in detail in Chap. 4. The burning rate is also dependent on the surface type, that is, if a fuel spillage is released onto a hard asphalt surface or onto a surface with a layer of macadam as is often used in rail tunnels.

Lönnermark et al. [21] performed a test series to study the effect of the relation between the fuel height and macadam on the burning rate. The test series, performed with different depth of liquid fuel (heptane and diesel) in a pool with macadam, showed that the macadam had a significant influence on the burning rate of the fuel.

The fire tests were performed using a pool with an area of 3.1 m^2 (2 m diameter). The pool was placed beneath an industry calorimeter to measure the HRR. Macadam was included in the pool up to a height of 0.15 m. Railway macadam of Class I (washed; 32–64 mm) was used. The bulk volume of the macadam was approximately half the free volume of the pool with the same height, that is, half the amount of liquid could be used to reach the same height in the pool compared to the case without macadam in the pool.

Heptane was used as the main fuel. During the test series the volume and depth of fuel were varied. The main parameter varied was the depth of fuel in relation to the depth of macadam, that is, the level of the upper surface of the fuel in relation to the upper layer of the macadam. To limit the time for each test, a water layer was added beneath the fuel in the pool. Two tests were also performed with diesel oil as fuel to study the influence of the fuel characteristics on the results. For each fuel a free-burning test without macadam was performed.

From the analyses it can be seen that the HRR for all cases with macadam are affected relative to the free-burning cases. When the upper fuel level is a distance below the upper macadam level there is a significant effect. This effect increases with the distance between the fuel surface and the upper level of macadam. This is shown graphically in Fig. 11.4. The influence of macadam can be used in rail tunnels or in other situation with macadam where the effect of a fuel release should be assessed.

11.3 Fire Spread in Tunnels

The different ways of fire spread in a tunnel were presented in Sect. 11.1:

1. Flame impingement
2. Flame spread
3. Remote ignition
4. Fuel transfer
5. Explosion.

Some of these points have been briefly discussed as separate issues in the sections above. In this section, the specific situation with a fire in a tunnel and ways and

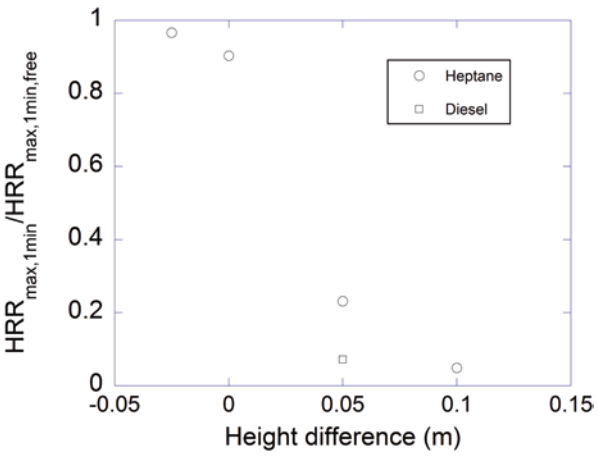

Fig. 11.4 The ratio between the peak 1 min average of the HRR for tests with macadam and a free-burning test without macadam, presented as function of the height difference between the level of macadam and the level of the *upper* surface of the liquid fuel. A positive height difference indicates the liquid surface is *below* the level of macadam

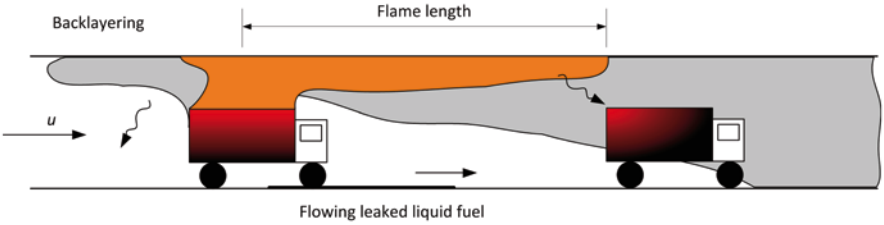

Fig. 11.5 Examples of different processes in fire spread in a tunnel

consequences of fire spread are discussed. In Fig. 11.5 some of the ways of fire spread given in the list above are exemplified.

The specific geometry of a tunnel with its *semi-confined* space with walls and often very limited ceiling height makes the fire spread situation very much different from fires freely burning above ground. Initially, the fire starts to spread inside the vehicle and the flames and hot gases extend to the ceiling. With limited ventilation the flames and hot gases are then guided in two directions along the tunnel tube. If a significant ventilation flow is present, the flames and fire gases are directed in mainly one direction. The extent of the flow of hot gases depends on the type of ventilation system and where the extraction points are positioned (see Chap. 13).

In road tunnels the main reasons for large fires are collisions between vehicles or with the tunnel wall. In the latter case, the vehicle can catch fire directly or due to subsequent collision with other vehicles. Some other causes are overheating (engine, brakes), faults in the engine or gear box, leakage of flammable liquids, etc.

A stop in a tunnel, due to a single-vehicle stop or collision, often results in a long queue of vehicle or even a multivehicle pileup, which could lead to further fire spread. This is also the situation if there is a queue downstream of the fire as well. This could be the case in a city tunnel during rush hours or because of a stop in the traffic due to another accident.

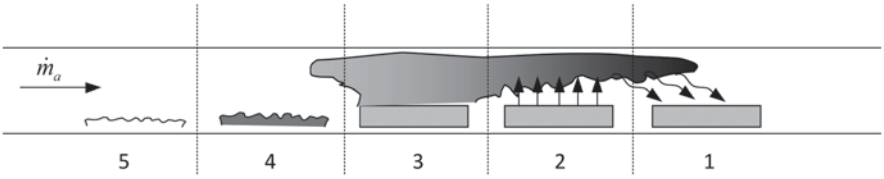

Fig. 11.6 Schematic description of the fire spread and burning process in a ventilation controlled fire in a tunnel. (After Ingason [22])

The main reasons for fires in rail tunnel are not as obvious as those in road tunnels. There are, however, fires due to collisions also in rail tunnels. Furthermore, derailment is the cause of several fires. In some cases the event has started with an explosion. Some have electrical causes, not only underneath the train (for example, due to short circuit) but also inside the train, for example, in a cabinet. Some causes are not fully described while several were due to arson. Examples of key fire incidents in rail tunnels are given in Chap. 1.

In many cases, fires in tunnels are not ventilation controlled, but if there are several vehicles involved in the fire a ventilation-controlled situation can occur. The fire spread and burning process in such a situation is schematically presented in Fig. 11.6. The process can be divided into five different steps as shown in the figure:

1. Preheating of unburnt fuel downstream of the fire
2. Pyrolysis leading to a region with excess fuel
3. Combustion (fully-developed fire)
4. Glowing ember
5. Burnt out/cooling

If there are more vehicles positioned further downstream in the tunnel the described process will continue and move in the downstream direction in the tunnel, starting from point 1 again.

If the fire is assumed to radiate as a point source, the radiation from the fire can be estimated by

$$\dot{q}'' = \frac{\chi_r \dot{Q}}{4\pi r^2} = K_r \frac{\dot{Q}}{r^2} \tag{11.17}$$

where χ_r is the fraction of the total HRR, $\dot{Q}$ (kW), that is emitted as radiation and K_r is a constant based on χ_r. In Table 11.6 χ_r and K_r are given for some selected materials. For the gases and several of the liquids the average of χ_r is approximately 0.3, which is a value commonly used. However, as seen in the table, the values vary from 0.14 for methane upto 0.64 for one of the rigid PU foams. Also some of the liquids have high values. Therefore, it is important not to use 0.3 in all situations, but try to relate the value to what is actually burning. The average for all the values of χ_r in the table is 0.40 (53 different materials), but this value of course depends on what materials are included. One should, however, note that the data were obtained from small-scale tests which differ from large-scale fires. Full-scale test data are recommended for use if they are available. For many of the common hydrocarbon

Table 11.6 Radiation fraction from different burning materials, calculated based on data from Tewarson [24]

Material	χ_r	K_r
Methane	0.14	0.011
Ethane	0.25	0.020
Propane	0.29	0.023
Butane	0.31	0.024
Ethylene	0.34	0.027
Propylene	0.37	0.029
Average common gases	0.28	0.022
Methyl alcohol	0.16	0.012
Ethyl alcohol	0.25	0.020
Isopropyl alcohol	0.29	0.023
Acetone	0.27	0.022
Heptane	0.33	0.026
Octane	0.33	0.027
Kerosene	0.35	0.028
Benzene	0.60	0.048
Toluene	0.60	0.047
Styrene	0.53	0.042
Average common liquids	0.37	0.030
Tissue paper	0.41	0.033
Wood (red oak)	0.37	0.030
Wood (Douglas fir)	0.38	0.030
Wood (pine)	0.30	0.024
Average cellulosic materials	0.36	0.029
POM	0.22	0.018
PMMA	0.31	0.025
PE	0.43	0.034
PP	0.41	0.033
PS	0.59	0.047
Silicone	0.31	0.025
Polyester-1	0.48	0.038
Nylon	0.40	0.032
Average synthetic solids	0.40	0.031
PU (flexible) foam GM21	0.52	0.041
PU (flexible) foam GM23	0.46	0.036
PU (flexible) foam GM25	0.58	0.046
PU (flexible) foam GM27	0.54	0.043
Average flexible PU foams	0.52	0.042
PUR (rigid) foam GM29	0.59	0.047

Table 11.6 (continued)

Material	χ_r	K_r
PU (rigid) foam GM31	0.55	0.044
PU (rigid) foam GM35	0.56	0.044
PU (rigid) foam GM37	0.51	0.041
PU (rigid) foam GM41	0.64	0.051
PU (rigid) foam GM43	0.57	0.045
Average rigid PU foams	0.57	0.045
PS foam GM47	0.56	0.045
PS foam GM49	0.61	0.049
PS foam GM51	0.58	0.046
PS foam GM53	0.57	0.045
Average PS foams	0.58	0.046
Corrugated paper boxes, empty	0.25	0.020
Corrugated paper boxes w. PVC (62 %-thick)	0.11	0.009
Corrugated paper boxes w. PC (59 %-thick)	0.27	0.021
Corrugated paper boxes w. PS (58 %-thick)	0.23	0.018
Corrugated paper boxes w. PS (60 %-thin)	0.48	0.038
Corrugated paper boxes w. PS (40 %-thin)	0.36	0.029
Corrugated paper boxes w. ABS (59 %-thick)	0.21	0.017
Corrugated paper boxes w. PET (41 %-thin)	0.41	0.032
Corrugated paper boxes w. PU (40 %-foam)	0.40	0.032
Average corrugated paper boxes w/wo polymers	0.30	0.024

fuels the radiative fraction decreases with increasing pool diameter. Koseki [23] reports that when the fire diameter is smaller than about 2 m, the radiative fraction for these fuels is 0.3–0.5, while when increasing the diameter to 10 m the radiative fraction decreases to 0.07–0.2. Further, note that the assumption that a fire is a radiation point source is a simplification that can be useful in some situations to estimate the risk for fire spread. However, in other situations a more detailed analysis is needed, for example, when there are long flames radiating toward an object. For information on more general methods for calculating radiation, see Chap. 10.

Large-scale tests simulating HGV fires were performed in the Runehamar tunnel, 2003 [25]. The radiation given by Eq. (11.17) was calculated for the maximum HRR during the mentioned Runehamar tests. The values were measured on the upstream side of the fire. In Fig. 11.7 these calculated values were compared to measured values [26]. In these calculations, a value of 0.3 was used for χ_r. A relatively good correlation can be seen.

In the tests in the Runehamar tunnel, fire spread was studied using targets downstream of a mock-up simulating an HGV fire [27]. Different types of targets were used: large targets with the same type of commodity as used in each of the full-scale tests and smaller wooden and plastic targets placed on the ground at different dis-

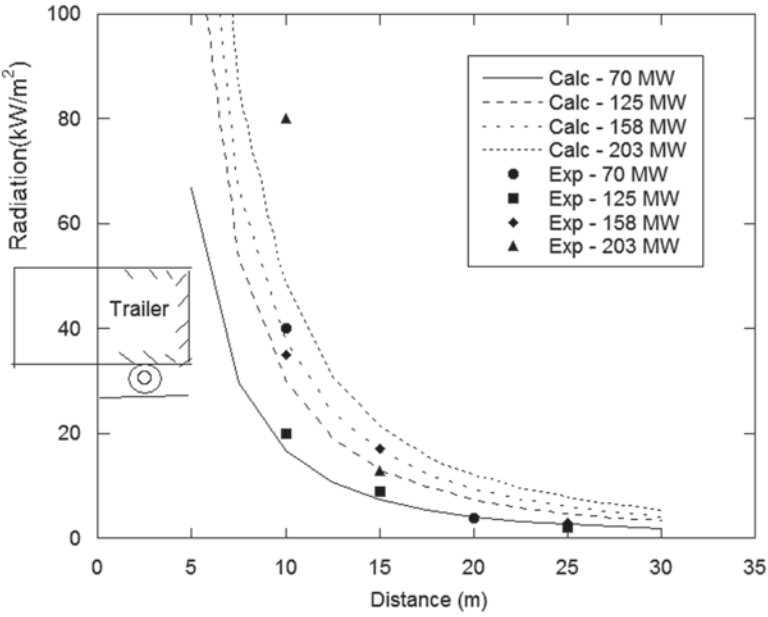

Fig. 11.7 Calculated (*Calc*) and experimental (*Exp*) radiation levels upstream of experimental setup in the Runehamar tests. The calculated values are based on the maximum HRR and the distance from the center of the fire (trailer mock-up) [26]

tances from the seat of the fire. The plastic targets were affected approximately up to the flame length while the fire spread to the pieces of wood occurred up to a distance of about (or somewhat more than) 70 % of the flame length. For the 202 MW fire in test T1 this corresponds to fire spread distances of 95 m for plastic targets and 70 m for wooden targets. This corresponds to spontaneous ignition due to radiation dominated fire spread from the upper layer to the road surface. With a higher target, for example, a vehicle with a cargo, the fire might spread even further distances between the initial fire and the target since convective heating and high temperature in the upper layer influence the target to a larger extent. Also direct impingement of flames onto the target can occur. The radiation will, however, still be an important factor for the fire spread. When the fire spreads to the large target (20–22 m downstream of the center of the fire), the HRR was in the range of 20–40 MW. This was obtained in a longitudinal flow of about 2–3 m/s.

The fire spread results from the Runehamar tests can be compared to the observations from the fire in the Fréjus tunnel in June 2005. The fire started in the engine of an HGV loaded with tyres [28]. The fire then spreads to an HGV loaded with cheese 60 m away. An HGV with scrap metal another 60 m away was also ignited. A fourth HGV, 350 m from the initial fire was ignited, but this was extinguished before the tank containing toxic glue was ruptured [29]. This HGV was extinguished approximately 6 h after the driver of the first HGV pressed the SOS button [28]. These observations correlate well with the results from the Runehamar tests. It

shows the long distances this type of fire can spread and, once again emphasizes the importance of HGVs on the outcome of tunnel fires.

A number of road tunnels fires have occurred throughout Europe with catastrophic results. These are described in Chap. 1, Tables 1.1 and 1.2. In all these fires, the cargo in HGV trailers played a major role in the outcome. The main reason being that the trailers contain a very high-fire load and the fire could easily spread within the cargo and further to adjacent vehicles due to the tunnel ventilation and the long flames created. Fire spread between vehicles is, therefore, of great concern inside a tunnel. An interesting thing to note is that, typically, fires involving only one HGV lead to no fatalities. There are many such examples, for example, Fréjus 1983, St. Gotthard 1984, Fréjus 1993, St. Gotthard 1994, and St. Gotthard 1997. On the other hand as soon as two or more HGVs are involved, the severity of the situation increases leading to fatalities, for example, in Velsen 1978, Nihonzaka 1979, Gumefens 1987, Serra a Ripoli 1993, St. Gotthard 2001, and Fréjus 2005. One important exception is the fire in the Channel tunnel in 1996, which involved in total ten HGVs, but did not lead to any fatalities. However, there are some important features of this fire that make it different. The HGVs were transported on a train and all the drivers and other people travelling on the train were sitting in a special passenger coach in the front of the train. With a supplementary ventilation system, the operator managed to reverse the air flow making the fire spread in the opposite direction. This made it possible for the people to escape with only minor effects of the smoke.

It can be worth noting that both in the St. Gotthard tunnel, where one of the catastrophic fires occurred, and in the Fréjus tunnel with fatalities during a fire in 2005, there have previously been fires not leading to fatalities and the main difference between these cases seems to be the number of HGVs. In the St. Gotthard tunnel HGVs/lorries were involved in fires on 14 separate occasions between 1992 and 1998 [30].

The analysis of the fires in tunnels presented in Tables 1.1 and 1.2 showed the importance of the number of vehicles involved in a fire, and even when the number of HGVs involved in a fire in a tunnel increased from one to two, the risk for a catastrophic outcome seems to increase significantly. This underlines the importance of fire spread for the severity of a fire in a tunnel. In the Mont Blanc tunnel fire in 1999, a total of 15 HGVs entering from the French side were burnt over a distance of 500 m (another 8 HGVs entering from the Italian side were also involved in the fire) [31, 32]. The distance between the HGVs varied between 3 and 45 m. In the fire in the St. Gotthard tunnel 2001, 13 HGVs and 10 cars over a distance of 550 m were involved in the fire.

There are several reasons why the fire spread and involvement of more than one vehicle are important for the outcome of the fire. One reason is that as soon as two or more vehicles are involved it can be very difficult for the rescue services to reach the site of the fire, both due to the increased radiation and to the fact that the rescue services would need to be able to come between the burning vehicles to be able to fight the fire. The ventilation can have a crucial impact on this situation since ventilation can make the conditions upstream of the first vehicle endurable for the rescue

services approaching the fire, while the conditions downstream of the first vehicle can become more severe and the fire can spread more easily.

One conclusion from fires in tunnels presented and discussed above is that goods that are considered to be nonhazardous transported on an HGV must be considered to be hazardous when involved in a fire in a tunnel. As soon as more than one HGV is involved in a fire in a tunnel, the situation becomes severe and often leads to fatalities. Both real fires in tunnels and fire experiments have shown that there are risks of fire spread over long distances when HGVs are involved in the fire.

Example 11.2 A HGV trailer carrying tissue paper is burning. The peak HRR is estimated to be 75 MW. How close to the fire can the fire fighters reach if their protecting clothes can withstand 5 kW/m^2 during their operation?

Solution: We rearrange Eq. (11.17) *to obtain the distance r. This means that* $r = \sqrt{K_r \frac{\dot{Q}}{\dot{q}''}}$ *. We obtain* K_r *from* Table 11.6 *for tissue paper,* $K_r = 0.033$*. Thus, the critical distance for the fire fighters is* $\sqrt{0.033 \frac{75000}{5}} = 22$ *m.*

11.4 Modeling of Fire Spread

Much of the modeling performed for tunnels include CFD modeling to calculate the temperature distribution and flow of hot gases and smoke (see Chap. 17). It is possible to use results from such models or from hand calculations to estimate the risk for fire spread, for example, by estimating the radiation (see for example, Sect. 11.3).

Ignition of a solid, however, involves many different processes and it can be difficult to model in detail. It is, therefore, common to make a number of assumptions and simplifications to be able to derive an equation that is possible to solve. In addition, many of those expressions are related to a specific test method with controlled conditions. The most common representations and assumptions for piloted ignition of solids are presented and discussed by Torero [33] and Babrauskas [2].

The main assumptions are:

- The solid remains inert until ignition, that is, the time delay before ignition is mainly related to heating the solid. This means that ignition will occur at the onset of pyrolysis. The ignition process can be represented by an ignition temperature T_{ig} (surface temperature at ignition) and an ignition delay time, t_{ig} (s), which is the time delay from start of exposure to ignition.
- Constant thermal material properties, both in space and time, that is, for k (kW/(m K)), ρ (kg/m^3), and c (kJ/(kg K)).
- Most of the incident heat flux, $\dot{q}_e''$ (kW/m^2), is absorbed by the solid at the surface, that is, absorptance $\alpha_r \approx 1$.
- Linearizing of the surface radiation and lumping the reradiation term together with the convective term using a total or effective heat transfer coefficient, h_{eff} (kW/(m^2 K)).

- Assumptions regarding the backside losses, for example semi-infinite (thermally-thick body)

Note that Torero uses the name minimum heat flux for ignition while Babrauskas denotes it as critical heat flux, $\dot{q}''_{cr}$ (kW/m^2). Babrauskas describes that there actually is a minimum heat flux $\dot{q}''_{\min}$ (higher than $\dot{q}''_{cr}$) at the time of ignition below which ignition does not occur. This means that there is a finite maximum t_{ig} for ignition to occur. Still, if it is assumed that $t_{ig} \to \infty$ (under the critical condition), the following equation can be derived:

$$T_{ig} = T_0 + \frac{\dot{q}''_{cr}}{h_{eff}} \tag{11.18}$$

Assuming a constant external heat flux, the following equation for the case with high-incident heat flux can be derived [33] (see also Chap. 10):

$$\frac{1}{\sqrt{t_{ig}}} = \frac{2}{\sqrt{\pi}\sqrt{k\rho c}} \frac{\dot{q}''_e}{\left(T_{ig} - T_0\right)} \tag{11.19}$$

This case is valid for $t_{ig} << t_c$, where

$$t_c = \frac{k\rho c}{h_{eff}^2} \tag{11.20}$$

The corresponding equation for a case with low incident heat flux ($t_{ig} \geq t_c$) [33]:

$$\frac{1}{\sqrt{t_{ig}}} = \frac{\sqrt{\pi}\sqrt{k\rho c}}{h_{eff}} \left[1 - \frac{h_{eff}\left(T_{ig} - T_0\right)}{\dot{q}''_e}\right] \tag{11.21}$$

To correlate the derived equation with experimental results different procedures and relations have been suggested. Janssens derived the following equation [2]:

$$\dot{q}''_e = \dot{q}''_{cr} \left[1 + 0.73 \left(\frac{k\rho c}{h_{eff}^2 t_{ig}}\right)^{0.55}\right] \tag{11.22}$$

Note the different exponent of the thermal inertia and t_{ig}.

The ignition time delay can from Eq. (11.22) be written as:

$$t_{ig} = \frac{0.56 \cdot k\rho c}{h_{eff}^2 \left[\frac{\dot{q}''_e}{\dot{q}''_{cr}} - 1\right]^{1.82}} \tag{11.23}$$

For thermally thin solids Babrauskas presents three different cases where the front face in all cases is exposed to radiant heat flux and there is re-radiation and convective cooling:

1. The back face is perfectly insulated.
2. The back face undergoes reradiation and convective cooling.
3. The back face is exposed to identical heat flux as the front face and undergoes reradiation and convective cooling

Note that for the discussions above, piloted ignition has been assumed. For cases without pilot, the air velocity and temperature strongly affect the time to ignition. This is extensively discussed by Babrauskas [2].

For tunnels the situations in many cases are extreme and significantly different from the conditions in the different test methods used when determining values for, for example, $\dot{q}''_{cr}$. The high air flow around the object for the fire to spread to may cool and disperse the mixture of pyrolysis gases at the surface and thereby delay the ignition process. Therefore, much care must be taken when taking these values into a real tunnel fire situation. However, the table values presented in this chapter together with the presented equation can give information on important influencing factors and relative differences between various materials.

One of the few models specifically developed for fire spread in tunnels is the one developed by Beard [34–38]. The model (FIRE-SPRINT) was created to model the fire spread from a burning HGV to a second HGV. There has been a continuous development of the model through different versions as summarized below (if nothing is mentioned the next version of the model has the same assumptions as the one before):

FIRE-SPRINT A1 [34]: It was assumed that the fire does not extend over or around the target vehicle, but is retained near the region of the initially burning vehicle (no flames extend downstream of the initial fire). A flow of air of ambient temperature exists in the tunnel due to forced ventilation. No smoke is assumed to move upstream. No radiative heat transfer occurs from the fire to the gases, but radiative feedback exists on the fire from the gases.

FIRE-SPRINT A2 [35]: A flame is assumed to extend to the upper part of the tunnel, also above the target, but there is a region above the target with no flame (between the target and the flame). It is assumed that no direct radiative heat transfer occurs between the downstream flame and the target.

FIRE-SPRINT A3 [36]: As in FIRE-SPRINT A2, but with a thicker flame in the region between the fire and the target. Thermal radiation is assumed to exist between the downstream flame section and the top of the target object.

FIRE-SPRINT B1 [37]: Flame impingement onto the target is assumed to exist (a persistent flame impingement is assumed).

The models have been used to estimate the fire spread by calculating the limits of stability of the system (correlated with a jump in the temperature) by means of nonlinear dynamics, and investigating how these limits depend on the HRR, the air flow velocity and the distance between the fire and the target. In each of the above mentioned cases, the limit for HRR to reach an unstable condition (fire spread) has decreased, which is in line with what can be expected. For a case with 6.45 m distance between the fire and the target and an air velocity of 2 m/s, the critical value of the HRR was calculated to be 55.2, 45.3, 38.6, and 14 MW, respectively, for the four different model versions.

The differences in results obtained with the different versions show both the impact different processes can have on the results, and the importance of large-scale fire tests to validate both models used and assumptions made. There are also cases when flame impingement onto the target (for example, another vehicle) does not exist, which means that knowledge about the actual situation is needed to make the correct assumptions (that is, to choose the correct version of the fire spread model).

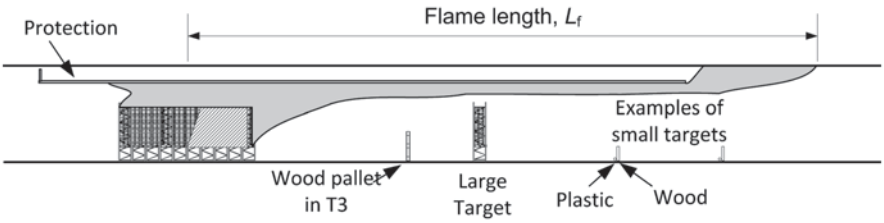

Fig. 11.8 A diagram of the fire load and the targets placed downstream of the fire. (From Lönnermark and Ingason [6])

To shed some light on the issue regarding whether flame impingement is probable during a certain fire situation or not, Carvel et al. [39] collected experimental information from the literature and used Bayes' Theorem to calculate the probability of impingement.

The authors scale the experimental results and draw the conclusion that the flames from a majority ("a large portion") of HGV fires will impinge on another HGV up to 20 m downstream of the fire. For a car fire (assumed to have a HRR less than 8 MW) it is unlikely that the flame will impinge on another vehicle more than 5 m downstream. In both cases the results are assumed to be valid for air velocities between 1 and 4 m/s.

Hansen and Ingason [40, 41] studied the fire risks in mines and developed a methodology to calculate fire spread among multiple objects to calculate HRR development in vehicles in underground structures. The modeling uses summation of individual HRR curves for different burning objects. The method, which was suggested by Ingason [42], is based on work by Numajiri and Furukawa [43]. It assumes a fire with a negligible constant period of maximum HRR and is useful only for fuel controlled fires. The model includes different parameters: maximum HRR, a retard index, an amplitude coefficient, and a time width coefficient. Several of these parameters can be related to the maximum HRR or the total energy content, but the retard index is determined by curve fitting. See Chap. 6 for further detailed information on fire curves.

To model fire spread it is also necessary to decide when a second object is ignited due to the flames from the first object. Three different methods to determine or model the ignition of a second object were evaluated as ignition criteria: one method with critical external heat flux and two methods using a surface ignition temperature. The first method was shown to be best for short distances between objects while the ignition temperature methods worked better for longer distances between the objects. Another issue is to find relevant values for critical heat flux and ignition temperatures as discussed earlier in the chapter. However, with suitable values good correlation can be found between the model and the experimental results for the selected scenarios.

Lönnermark and Ingason [27] investigated the fire spread in the Runehamar tests [25]. Several targets were placed at different locations downstream of the fire, see location of small targets of Plastic and Wood pieces at floor level in Fig. 11.8. Models of the average temperature for the cross-section were used to study the

connection of this parameter to fire spread. For the region of fire spread, a large temperature difference between the temperature in the upper layer and the calculated average temperature of the cross-section exists. This temperature difference has an important effect on the incident radiation, which in most cases is the cause of fire spread. The use of an average temperature in fire spread calculations might, therefore, be misleading.

In the vicinity of a fire, the radiation dominates the heat transfer. The incident heat flux represents the intensity of incident radiation from surroundings. The incident heat flux received on the target surface can be approximately estimated using the following equation (see Chap. 10 on heat flux):

$$\dot{q}''_{inc} = \varepsilon_g F_{o-g} \sigma T_g^4 \tag{11.24}$$

where ε_g is the gas emissivity, T_g is the gas temperature (K), $F_{o\text{-}g}$ is the view factor from the target to smoke layer. Note that T_g must be expressed in degrees Kelvin for this equation to be valid and ε_g in most cases can be considered as 1 for estimation of fire spread due to the sooty smoke layer. The view factor is equal to one if the target is immersed in the layer or else it is lower than 1, for example, a surface at the floor level. How to calculate this view factor can be found in Chap. 10 on heat flux.

The critical condition for ignition is difficult to identify. The critical ignition criterion varies significantly, including ignition temperature, critical heat flux, critical fuel mass flow rate, etc. In spite of the significant difference in determination of the critical ignition condition, it can be expected that there is a strong correlation between the ignition and the ceiling gas temperature in a ventilated tunnel fire. Ingason et al. [25] analyzed the ignition condition using the critical ceiling gas temperature, that is, the minimum ceiling gas temperature required to ignite the target material of plastic and wood material. At the ignition state, the controlling equation for the energy in the surface layer of the sample can be expressed as:

$$\dot{q}''_{ig} = \varepsilon_s (\dot{q}''_{inc,cr} - \sigma T_{ig}^4) + h_c (T_\infty - T_{ig}) \tag{11.25}$$

where $\dot{q}''_{ig}$ is the critical net heat flux at ignition (kW/m^2), $\dot{q}''_{inc,cr}$ is the critical incident heat flux at ignition (kW/m^2) from Eq. (11.24), ε_s is the surface emissivity of the sample and T_{ig} is the ignition temperature (K). Since the emissivities of the common materials, such as wood and PE plastic, are generally in a range of 0.8–0.95, the surface emissivity of the sample is not supposed to have a strong influence on the total heat flux absorbed by the sample, except for some special materials. The above equation in fact indicates that there exists a critical incident heat flux corresponding to the ignition state in a given condition.

Ingason et al. [25] found that the location of wood crib surface relative to the smoke layer height plays an important role in the fire spread. It can be argued that the fire spread to the second vehicle is unlikely to occur if a tunnel height is very high, say up to twice the vehicle height. They found that for wood the ceiling gas temperature at the edge of fire spread, that is, the critical ceiling gas temperature, is in a range of 709–955 °C in the Runehamar test T2, 674–740 °C in T3 and 674–740 °C in T4. This means that a ceiling gas temperature of about 700 °C is required to ignite the wood crib placed on the floor level. The mechanism of ignition should

be the spontaneous ignition by thermal radiation. According to Li et al. [44], a surface temperature of 600 °C should be obtained for wood before its spontaneous ignition. Given the differences between experimental conditions in the tunnel and those in the reference, these temperatures correlate well with each other. In a study of the fire spread using model scale tests [45], the critical ceiling gas temperature for fire spread to the second wood cribs is about 600 °C for fire spread to the wood with *surface close to the ceiling* in a tunnel fire. It is therefore concluded that the critical ceiling gas temperature is about 700 °C for fire spread to a wood *at floor level* and about 600 °C for fire spread to the wood with *surface closer to the ceiling (mid tunnel height)* in a tunnel fire.

For plastic material the critical ceiling gas temperature, is below 1001 °C in the Runehamar tunnel fire test T1, below 710 °C in T2, below 672 °C in T3 and in a range of 466–514 °C in T4. Compared to the wood, the plastic material in these tests was much easier to ignite. It was concluded that the critical ceiling gas temperature for fire spread to the plastic materials placed at the floor level can be considered to be 490 °C, that is, an average value of 466–514 °C in T4.

11.5 Summary

In the chapter different parameters affecting the ignition and fire spread are presented and discussed. For tunnels the situations in many cases are extreme and significantly different from the conditions in the test methods used when determining values, for example, $\dot{q}''_{cr}$. Therefore, much care must be taken when applying these values to a real tunnel fire situation. However, the table values presented in this chapter together with the presented equations can give information on important influencing factors and relative differences between various materials. A few fire spread models specifically developed for tunnels or vehicles are also presented.

It is also shown that ordinary cargo can be hazardous in tunnels, both due to fast developing and high HRR fire and due to the high risk for fire spread. The involvement of more than one HGV in a fire significantly increases the risk for severe outcomes, for example, fatalities. This emphasizes the importance of fire spread in tunnels and the effect on the fire development, possibilities for the fire and rescue services to fight the fire and on the final outcome of the fire.

References

1. Rew C, Deaves D Fire spread and flame length in ventilated tunnels—a model used in Channel tunnel assessments. In: Proceedings of the International Conference on Tunnel Fires and Escape from Tunnels, Lyon, France, 5–7 May 1999. Independent Technical Conferences Ltd, pp 397–406
2. Babrauskas V (2003) Ignition Handbook. Fire Science Publishers, Issaquah, WA, USA
3. Wickström U (To be published) Heat Transfer in Fire Technology. Draft 26 March 2013 edn.

4. Quintiere JG (1998) Principals of Fire Behavior. Delmar Publishers
5. Drysdale D (1994) An Introduction to Fire Dynamics. John Wiley & Sons
6. Kanury AM (1972) Ignition of cellulosic materials: a review. Fire Research Abstracts and Reviews 14:24–52
7. Dillon SE (1998) Analysis of the ISO9705 Rom/Corner Test: Simulations, Correlations and Heat Flux Measurements M.S. Thesis, Department of Fire Protection Engineering, University of Maryland
8. Cleary TG, Quintiere JG (1991) Flammability Characterization of Foam Plastics. NIST
9. Hopkins Dj, Quintiere JG (1996) Material Fire Properties and Predictions for Thermoplastics. Fire Safety Journal 26:241–268
10. Grexa O, Janssens M, White R, Dietenberger M Fundamental Thermophysical Prperties of Materials Derived from Cone Calorimeter Measurements. In: Wood & Fire Safety: 3rd International Scientific Conference, 1998. The High Tatras, Slovak Republic, pp 139–147
11. Henderson A (1998) Predicting Ignition Time under Transient Heat Flux Using Results from Constant Heat Flux Experiments. School of Engineering, Univ. Canterbury, Christchurch, New Zealand
12. Janssens ML (1991) Fundamental Thermophysical Characteristics of Wood and Their Role in Enclosure Fire Growth. Ph.D dissertation, University of Gent, Belgium
13. Harkleroad M. Unpublished NIST data
14. Grexa O, Horváthová E, Osvald A Cone Calorimeter Studies of Wood Species. In: International Symposium on Fire Science and Technology, Seoul, 1997. Korean Institute of Fire Science & Enginering, pp 77–84
15. Dietenberger M, Grexa O Analytical Model of Flame Spread in Full-scale Room/Corner Tests (ISO 9705). In: Fire & Materials ’99, 6th International Conference, 1999. Interscience Communications Ltd, pp 211–222
16. NFPA (1981) NFPA Handbook. National Fire Protection Association
17. Glassman I, Dryer F (1980/81) Flame spreading across liquid fuels. Fire Safety Journal 3:123–138
18. Gottuk DT, White DA (2008) Liquid Fuel Fires. In: DiNenno P (ed) The SFPE Handbook of Fire Protection Engineering. Quincy: National Fire Protection Association, pp 2–337 – 332–357
19. Ingason H Small Scale Test of a Road Tanker Fire. In: Ivarson E (ed) International Conference on Fires in Tunnels, Borås, Sweden, October 10–11 1994. SP Swedish National Testing and Research Institute, pp pp. 238–248
20. White D, et al. (1997) Flame Spread on Aviation Fuels Fire Safety Journal Volume 28:pp. 1–31
21. Lönnermark A, Kristensson P, Helltegen M, Bobert M Fire suppression and structure protection for cargo train tunnels: Macadam and HotFoam. In: Lönnermark A, Ingason H (eds) 3rd International Symposium on Safety and Security in Tunnels (ISTSS 2008), Stockholm, Sweden, 12–14 March 2008. SP Technical Research Institute of Sweden, pp 217–228
22. Ingason H (2012) Fire Dynamics in Tunnels. In: Beard AN, Carvel RO (eds) In The Handbook of Tunnel Fire Safety, 2nd Edition ICE Publishing, London, pp 273–304
23. Koseki H (1989) Combustion Properties of Large Liquid Pool Fires. Fire Technology 25 (August):241–255
24. Tewardson A (2008) Generation of Heat and Gaseous, Liquid, and Solid Products in Fires. In: DiNenno PJ, Drysdale D, Beyler CL et al. (eds) The SFPE Handbook of Fire Protection Engineering. Fourth Edition edn. National Fire Protection Association, Quincy, MA, USA, pp 3–109–103–194
25. Ingason H, Lönnermark A, Li YZ (2011) Runehamar Tunnel Fire Tests. SP Technicial Research Institute, SP Report 2011:55
26. Ingason H, Bergqvist A, Lönnermark A, Frantzich H, Hasselrot K (2005) Räddningsinsatser i vägtunnlar. Räddningsverket, P21-459/05 (in Swedish)
27. Lönnermark A, Ingason H (2006) Fire Spread and Flame Length in Large-Scale Tunnel Fires. Fire Technology 42 (4):283–302

28. BEA-TT (2006) Rapport provisoire d'enquête technique sur l'incendie de poids lours survenu dans le tunnel du Fréjus le 4 juin 2005. Bureau d'Enquêtes sur les Accidents de Transport Terrestre, France
29. Brinson A (2005) Fire in French Tunnel Kills Two. Eurosprinkler
30. Bettelini M, Neuenschwander H, Henke A, Gagliardi M, Steiner W The Fire in the St Gotthard Tunnel of October 24, 2001. In: Ingason H (ed) International Symposium on Catastrophic Tunnel Fires (CTF), Borås, Sweden, 20–21 November 2003. SP Swedish National Testing and Research Institute, pp 49–68
31. Ingason H Fire Development in Catastrophic Tunnel Fires (CTF). In: Ingason H (ed) International Symposium on Catastrophic Tunnel Fires (CTF), Borås, Sweden, 20–21 November 2003. SP Swedish National Testing and Research Institute, pp 31–47
32. Duffé P, Marec M (1999) Report on the Technical Enquiry into the Fire on 24 March 1999 in the Mont Blanc Tunnel. Ministry of the Interior, Ministry for Equipment, Transport and Accommodation, France
33. Torero JL (2008) Flaming Ignition of Solid Fuels. In: DiNenno P (ed) The SFPE Handbook of Fire Protection Engineering. Quincy: National Fire Protection Association, pp 2–260 – 262–277
34. Beard AN, Drysdale DD, Bishop SR (1995) A Non-linear Model of Major Fire Spread in a Tunnel. Fire Safety Journal 24:333–357
35. Beard AN (1997) A Model for Predicting Fire Spread in Tunnels. Journal of Fire Sciences 15 (July/August):277–307
36. Beard AN Major Fire Spread in a Tunnel: A Non-linear Model. In: Vardy AE (ed) Fourth International Conference on Safety in Road and Rail Tunnels, Madrid, Spain, 2–6 April 2001. University of Dundee and Independent Technical Conferences Ltd., pp 467–476
37. Beard AN Major Fire Spread in a Tunnel: A Non-linear Model with Flame Impingement. In: Proceedings of the 5th International Conference on Safety in Road and Rail Tunnels, Marseille, France, 6–10 October 2003. University of Dundee and Independent Technical Conferences Ltd., pp 511–521
38. Beard AN Major Fire Spread in a Tunnel, Assuming Flame Impingement: Effect of Separation and Ventilation Velocity. In: Fifth International Conference on Tunnel Fires, London, UK, 25–27 October 2004. Tunnel Management International, pp 317–326
39. Carvel RO, Beard AN, Jowitt PW The Influence of Longitudinal Ventilation on Fire Spread between HGV Fires in Tunnels. In: Fifth International Conference on Tunnel Fires, London, UK, 25–27 October 2004. Tunnel Management International, pp 307–316
40. Hansen R, Ingason H (2011) An Engineering tool to calculate heat release rates of multiple objects in underground structures. Fire Safety Journal 46 (4):194–203. doi:10.1016/j.firesaf.2011.02.001
41. Hansen R, Ingason H (2012) Heat release rates of multiple objects at varying distances. Fire Safety Journal 52:1–10
42. Ingason H (2009) Design fire curves in tunnels. Fire Safety Journal 44 (2):259–265. doi:10.1016/j.firesaf.2008.06.009
43. Numajiri F, Furukawa K (1998) Short Communication: Mathematical Expression of Heat Release Rate Curve and Proposal of 'Burning Index'. Fire and Materials 22:39–42
44. Li YZ, Lei B, Ingason H (2011) The maximum temperature of buoyancy-driven smoke flow beneath the ceiling in tunnel fires. Fire Safety Journal 46 (4):204–210
45. Ingason H, Li YZ (2011) Model scale tunnel fire tests with point extraction ventilation. Journal of Fire Protection Engineering 21 (1):5–36